# QCT RECONSTRUCTION KERNEL HAS IMPORTANT QUANTITATIVE EFFECTS ON FINITE ELEMENT ESTIMATED BONE STRENGTH

Andrew S. Michalski [a, b], W. Brent Edwards [b, c], Steven K. Boyd [a, b]

[a] *Department of Radiology, Cumming School of Medicine;* [b] *McCaig Institute for Bone and Joint Health;* [c] *Faculty of Kinesiology, University of Calgary, Calgary, AB, Canada*

## INTRODUCTION

Osteoporosis is a common musculoskeletal disorder that specifically affects bone tissue and is characterized by overall poor bone quality, bone fragility, and increased fracture risk [1]. Osteoporosis is typically diagnosed by measuring the areal bone mineral density via dual energy X-ray absorptiometry (DXA). Areal bone mineral density measures of 2.5 standard deviations below the mean from the reference population are classified as osteoporotic. These measures are good predictors of fracture in osteoporotic populations, but they often fail to predict bone mechanical properties for an individual [2], and, as previous studies have shown, high rates of fragility fractures occur in groups not classified as osteoporotic via DXA [3, 4]. With these limitations of DXA, quantitative computed tomography (QCT) has been considered as an alternative to measure three-dimensional (3D) volumetric bone mineral density, and bone mineral content. QCT is often combined with finite element analysis (QCT-FE) to predict bone strength and fracture risk. QCT-FE methods have been validated through experimental mechanical testing [5, 6] and have also been shown to be computationally efficient [7].

To perform QCT-FE, the material properties of bone are derived by converting Hounsfield Units (HU) at each voxel to an apparent density value by using a linear relationship based on a density calibration phantom. Each density weighted voxel then can be converted to a Young's modulus based on empirical equation, such as [8]:

$$E = 10.50\rho_{ash}^{2.29} \tag{1}$$

where $\rho_{ash}$ is the calibrated density values in, and $E$ is the Young's modulus. There are several density-to-modulus relationships defined in the literature, but no matter which is applied, the determination of the Young's modulus can be influenced by the QCT acquisition and reconstruction, leading to imprecise bone strength, stiffness, and fracture risk prediction [6] when applied in the finite element method.

The filtered back projection CT reconstruction method is a standard algorithm to create CT images from the raw data of the scan. The filtered back-projection algorithms can use a variety convolution kernels, where each kernel applies a specific type of filter to the data during reconstruction. The B30 convolution kernel is a medium smoothing kernel, which applies a small amount of blurring to the data and suppresses some noise [9]. The B70 convolution kernel is a high sharpening kernel, which applies a high frequency filter to the data, enhancing edges in the data at the expense of increasing noise [9]. The B30 kernel is used typically for soft tissue viewing, while the B70 kernel is used specifically to view bone. Figure 1 depicts the plot profile along the line shown in red in the images, both reconstructed using different convolution kernels. The B70 sharpening kernel has a sharp change in HU at the edge, but this comes at the cost of increasing noise in the image. Whereas the B30 kernel plot profile has a more smooth change in HU, resulting from the increased blurring in the image. With increased usage of QCT-FE to assess bone strength and fracture risk in bone related research, the effect of reconstruction convolution kernel on the

outcomes of bone mineral density and bone strength needs to be further explored.

The purpose of this study was to determine the effects of QCT reconstruction kernel on the quantitative assessment of bone quality. We hypothesize that the QCT reconstruction kernel affects the outcome measures of the volumetric bone mineral density, bone mineral content, and ultimately the finite element predicted bone strength.
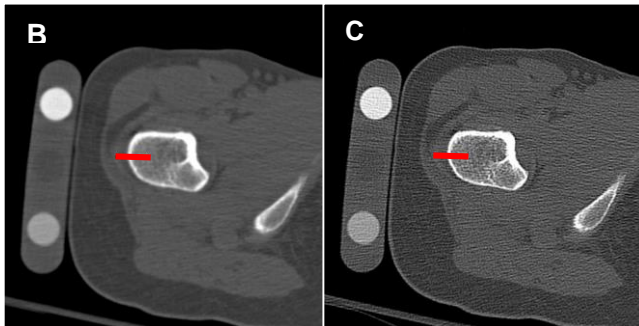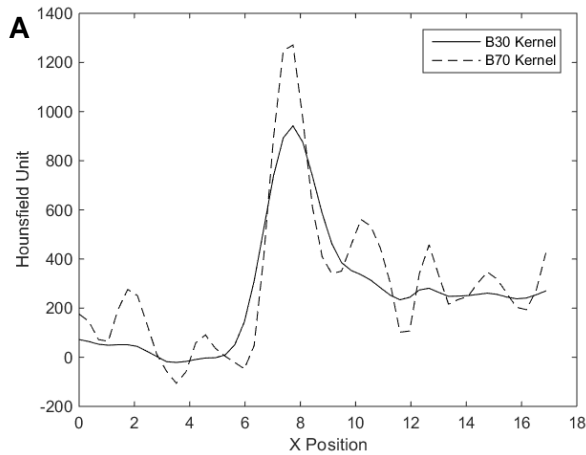


Figure 1: A) Profile plot of red lines from images in B and C. The B70 kernel image has increased noise at the edge intersection. B) Image of proximal femur, reconstructed using B30 convolution kernel. C) Image of proximal femur, reconstructed using B70 convolution kernel.

## MATERIALS AND METHODS

QCT Scan Acquisition

Twenty scans of the proximal were acquired from 14 subjects. The scans were performed using a Sensation 64 Cardiac (Siemens Medical Systems, Forccheim, Germany; 120 kVp, 280 mAs, pixel resolution 0.352 mm, slice thickness 1 mm). Each scan included a density calibration phantom with known calcium hydroxyapatite concentrations of 0.0, 0.4109, and 0.8169 g/cm$^3$

(QRM, Moehrendorf, Germany). The density calibration phantom provides a basis for Hounsfield Unit (HU) conversion to density values. Each scan was reconstructed using the standard (B30) kernel and the bone specific (B70) kernel.

Quantitative Bone Analysis

Bone mineral measurements were computed for the total proximal femur using both reconstruction kernels. Conversion of HU to density was performed using a linear calibration curve derived from measurements of the density calibration phantom included in the scan field of view. The proximal femur was segmented and analyzed using custom in house software developed utilizing the Visualization Toolkit (VTK 6.3; Kitware Inc.; Clifton Park, NY). A 0.15 g/cm$^3$ density threshold was used to acquire the surface boundary of the proximal femur; some manual identification was required to ensure proper segmentation of lower density regions of the proximal femur. Volumetric bone mineral density (vBMD; grams per cubic centimeter), bone mineral content (BMC; grams), and volume (cubic centimeters) were measured by including all voxels within the segmented regions. To prepare images for finite element analysis, density values were binned and assigned material IDs proportional to the CT image density. To account for varying bone strength with density, finite element models use a method introduced by Homminga [10] in which the moduli vary according to the equation,

$$E = E_{max}(\frac{\rho}{\rho_{max}})^x \qquad (2)$$

where $E_{max}$ is the defined elastic moduli, $\rho$ is the CT image density, and $x$ is the modulus exponent. Using the binned material IDs, equation 2 becomes

$$E = E_{max}(\frac{ID}{ID_{max}})^x \qquad (3)$$

where $ID$ is the assigned material ID based on binned CT image density for the corresponding voxel. Comparisons of measures between each

reconstruction kernel used a standard paired t-test. The criterion alpha-level was set to 0.05.

## RESULTS

QCT measures of bone mineral were determined for each scan using two reconstruction kernels, a clinical standard kernel (B30) and a bone specific kernel (B70). The measures for vBMD, BMC, and volume are illustrated in Figure 2. Measures of vBMD ($p < 0.001$) were significantly greater using the B70 reconstruction kernel. Measures of BMC ($p < 0.01$) and volume ($p < 0.001$) were significantly lower using the B70 reconstruction kernel. The max binned material ID ($p < 0.001$) was computed from each image and was significantly greater using the B70 reconstruction kernel, as depicted in Figure 3. The maximum material ID is related to the maximum density of the segmented bone. At the present time, no measure of finite element predicted bone strength has been performed; however, it is anticipated that the exponential relationship in equation 3 will impact the effective bone strength.

## DISCUSSION

The purpose of this study was to quantify the effects of CT reconstruction kernel on the assessment of vBMD, BMC, and finite element estimated bone strength. The findings illustrated that the bone specific kernel, B70, produced significantly higher measures of vBMD, and significantly lower measures of BMC and volume, as compared to the B30 kernel.

Some limitations to this study include the fact that only two reconstruction kernels were used, although there are many more kernels available. We selected the B30 kernel because it is a standard reconstruction, typically used for soft tissue visualization. The B70 kernel is a bone specific reconstruction kernel, which enhances edge definition in the image. Other kernels with varying amount of image sharpness are available. As the image sharpness increases, so does the image noise. The ideal reconstruction kernel for quantitative bone imaging may not be covered by the kernels used in this analysis. Furthermore, our analysis only examined differences in integral bone mineral of the
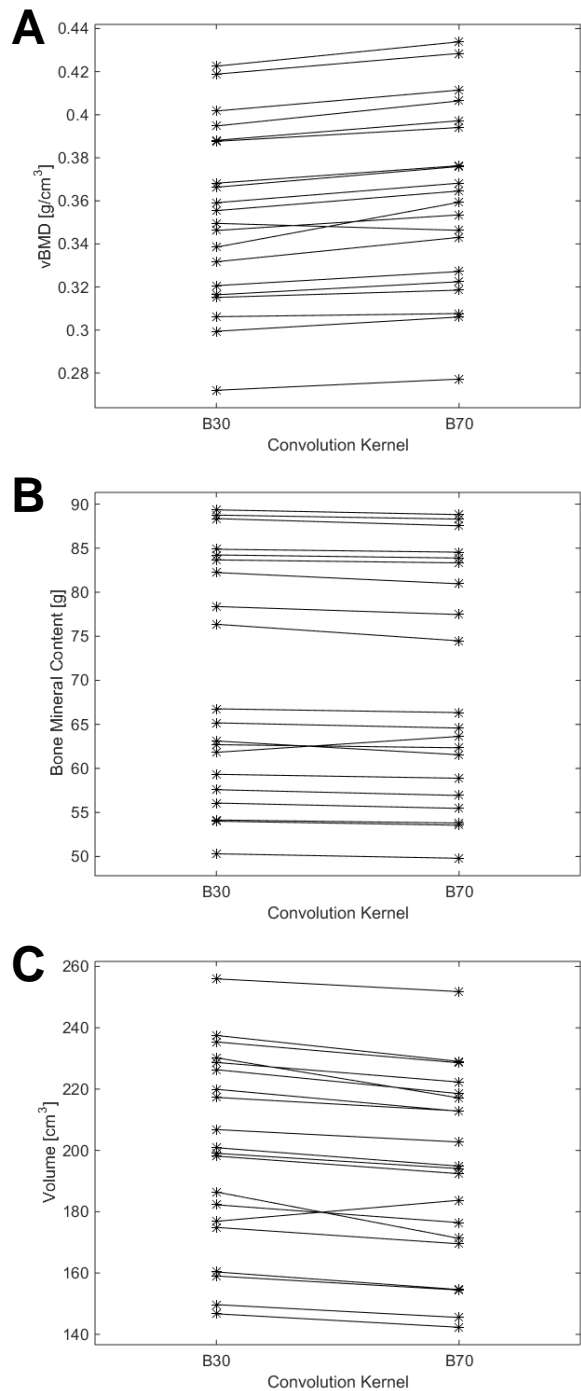


Figure 2: A) A significant increase using the B70 was found for the vBMD ($p < 0.001$). B) A significant decrease using the B70 kernel was found for the BMC measure ($p < 0.01$). C) A significant decrease using the B70 was found for the volume ($p < 0.001$).

proximal femur, which groups the cortical and trabecular bone regions together. Giambini *et al.* have shown that differences can be observed between cortical and trabecular region analysis. Using an *ex vivo* rabbit femur, images using the
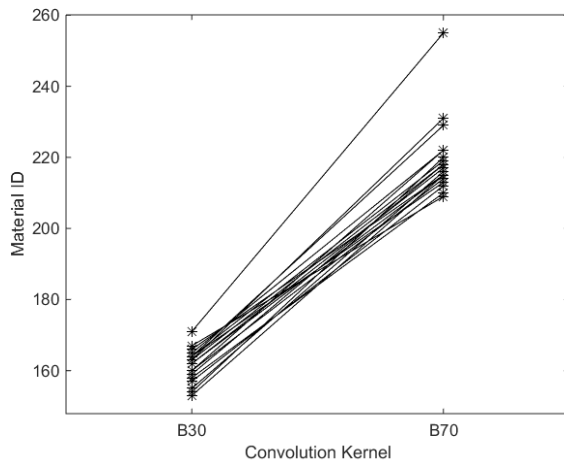
Figure 3: A significant increase in the maximum material ID (p < 0.001) was found. The maximum material is related to the maximum density of the segmented bone, which will have significant impact on finite element analysis.

B70 kernel had a higher vBMD in the cortical bone compared to images using the B30 kernel [11]. Conversely, the B70 reconstruction produced lower vBMD values in the trabecular bone region [11]. Further analysis is required to identify how these differences affect finite element outcomes. With increased density in the cortical bone, conversion to Young's moduli, using equation 3, could produce meaningful errors in FE estimated bone strength and stiffness. Such errors could lead to inaccurate results that may alter clinical assessment. Significant differences in the volume measures could be due to partial volume effects at bone-tissue interface. Segmentation methods could contribute to this error and thus influence the related measures of vBMD and BMC. Further study of segmentation method needs to be explored.

In order for QCT scanning to become a robust method for quantitative bone assessment, differences in vBMD need to be reduced or eliminated. Density calibration phantoms correct for current and voltage effects by the CT on the scan analysis, but do not address effects from the reconstruction kernel. Future work in analyzing the array of reconstruction kernels could allow for a general correction factor to be applied to the data to allow for inter-study data comparison, although a correction factor applied to compute vBMD measurements is not an ideal method. A standardized QCT acquisition protocol for quantitative bone imaging would be the ideal solution, which could be developed and adopted by the bone imaging community.

In summary, important significant differences in quantitative measures of bone quality between the B30 and B70 reconstruction convolution kernels were observed. These data illustrate that filtered back projection convolution kernel plays a significant role in quantitative measures of bone quality. The CT reconstruction kernel is an important factor to standardize in QCT acquisition and post-processing for future studies.

## REFERENCES

[1]     M. Kleerekoper, A.R. Villanueva, J. Stanciu, D. Sudhaker Rao, and A.M. Parfitt, "The role of three-dimensional trabecular microstructure in the pathogenesis of vertebral compression fractures," *Calcif Tis Int*, vol. 37, pp. 594 – 597, 1985.

[2]     M.L. Ciarelli, S.A. Goldstein, J.L. Kuhn, D.D. Cody, and M.B. Brown, "Evaluation of orthogonal mechanical properties and density of human trabecular bone from the major metaphyseal regions with materials testing and computed tomography," *J Orthop Res*, vol. 9, pp. 674 – 682, 1991.

[3]     C.S. Carlson, R.F. Loeser, M.J. Jayo, D.S. Weaver, M.R. Adams, and C.P. Jerome, "Osteoarthritis in cynomolgus macaques: a primate model of naturally occurring disease," *J Orthop Res*, vol. 12, pp. 331 – 339, 1994.

[4]     S.C.E. Schuit *et al.*, "Fracture incidence and association with bone mineral density in elderly men and women: the Rotterdam study," *Bone*, vol. 34, pp. 195 – 202, 2004.

[5]     J.H. Keyak, S.A. Rossi, K.A. Jones, and H.B. Skinner, "Prediction of femoral fracture load using automated finite element modeling," *J Biomech*, vol. 31, pp. 125 – 133, 1998.

[6]     D. Dragomir-Daescu, C. Salas, S. Uthamaraj, and T. Rossman, "Quantitative computed tomography-based finite element analysis predictions of femoral strength and stiffness depend on computed tomography settings," *J Biomech*, vol. 48, pp. 153 – 161, 2015.

[7]     K.K. Nishiyama, S. Gilchrist, P. Guy, P. Cripton, and S.K. Boyd, "Proximal femur bone strength estimated by a computationally fast finite element analysis in a sideways fall configuration," *J Biomech*, vol. 46, pp. 1231 – 1236, 2013.

[8]     T.S. Keller, "Predicting the compressive mechanical behavior of bone," *J Biomech*, vol. 27, pp. 1159 – 1168, 1994.

[9]     K.J. Jang *et al.*, "Measurement of image quality in CT images reconstructed with different kernels," *J Korean Phys Soc*, vol. 58, pp. 334 – 342, 2011.

[10]    J. Homminga, R. Huskies, B. Van Rietbergen, P. Rüegsegger, and H. Weinans, "Introduction and evaluation of a gray-value voxel conversion technique," *J Biomech*, vol. 34, pp. 513 – 517, 2001.

[11]    H. Giambini *et al.*, "The effect of quantitative computed tomography acquisition protocols on bone mineral density estimation," *J Biomech Eng*, vol. 137, 2015